III. MICROWAVE SPECTROSCOPY*

Academic and Research Staff

Prof. M. W. P. Strandberg
Prof. R. L. Kyhl
Dr. T. E. McEnally, Jr.
Dr. M. U. Palma
Dr. Maria B. Palma-Vittorelli
J. G. Ingersoll
J. D. Kierstead

Graduate Students

J. U. Free, Jr.
R. M. Langdon, Jr.
L. R. Fox
M. K. Maul
S. R. Reznek
B. N. Yung

RESEARCH OBJECTIVES

This group has a broad general interest in the study of metals and dielectric crystals by means of UHF and microwave frequency experiments with the use of electromagnetic and acoustic radiation. During the past year, the superconducting bolometric detector, developed for use with heat pulses (incoherent phonons), has been used to detect coherent phonons in a crystal rod. These bolometers can be made to be a linear detector of the acoustic power incident on them and, hence, are most suitable for studying the decay of the total coherent acoustic energy in the crystal without having to worry about the phase of the acoustic energy at the quartz surface, as is the case when using coherent detectors. Our studies of superconducting bolometers have indicated how they must be prepared for linear operation, and responsivity and noise measurements have been made by using them as microwave electromagnetic wave detectors. This work will continue.

Work has begun on measurements of acoustic absorption in metals to develop an understanding of the attenuation and boundary-layer thermal resistance at a metal-quartz interface. We have approximated with analytic functions the acoustic velocity surfaces appropriate to NaCl, quartz, and sapphire in the low-frequency limit. The representations will facilitate our understanding of heat-pulse propagation in these crystals, since they make analytic manipulation of the acoustic-wave properties relatively easy. This work will probably be finished in the coming year.

The research on the Fermi surface of gallium has been completed, and work has begun on the copper Fermi surface.

Other work which has been started and will continue is directed toward an analytical understanding of the electromagnetic properties of metals at low temperatures and in magnetic fields. Electron paramagnetic resonance studies of the cross-relaxation process in ruby have been finished and the results have been submitted for publication. A study of NMR signals in static electric fields has been completed. Apparatus designed to detect atomic hydrogen and hydrated electrons in aqueous samples has been completed. Thus far, the results have been negative. It is anticipated that this work will be finished early in the coming year.

Because of the interest of the Radio Astronomy Group in the CH free radical, we have developed very promising instrumentation for detection of CH in an EPR experiment in our laboratory, but these efforts are still inconclusive, and will probably continue for a short time also.

Work with the Department of Chemical Engineering, M.I.T., has been mainly directed at the calibration of a hydrogen atom detector, using the EPR apparatus as an instrument to measure quantitatively atomic hydrogen concentration. Research of a

*This work was supported by the Joint Services Electronics Programs (U.S. Army, U.S. Navy, and U.S. Air Force) under Contract DA 36-039-AMC-03200(E).

different sort, the measurements of chemical reaction-rate constants, is being prepared, also with this group, and will be carried out during the next year.

M. W. P. Strandberg, R. L. Kyhl

A. WORK COMPLETED

1. ELECTRIC FIELD EFFECTS IN THE NUCLEAR MAGNETIC RESONANCE OF FLUIDS

This research has been completed by Terence E. McEnally, Jr., and submitted as a thesis to the Department of Physics, M.I.T., August 1966, in partial fulfillment of the requirements for the degree of Doctor of Philosophy. A summary of the thesis follows.

When a molecule tumbles randomly with an orientational correlation time, τ, much less than the inverse of the linewidth, $\Delta\omega$, predicted for an ensemble of isolated, randomly oriented, nontumbling molecules, the NMR absorption lines become motionally narrowed, and the spectrum exhibits fine structure, because of interactions of the nuclei among themselves. Only the effects of the isotropic (zero-rank) parts of chemical shift and indirect spin-spin interaction tensors is usually observable, as their ranks 1 and 2 parts average to zero isotropically, as do the magnetic dipolar and electric quadrupolar tensors, which are both of rank 2. If the nonspherical molecule tumbles in a potential well of average nonspherical symmetry, then an orientational bias to the motion may ensue, without spoiling its motional narrowing properties. Then the 1^{st} and 2^{nd} rank parts of the nuclear interaction tensors may give an observable effect. Under the assumption of molecules at room temperature having nonzero electric dipole and/or quadrupole moments in a potential described by its first and second derivatives, the calculation of the orientational average of $D^{(\ell)}_{m'm}(\alpha\beta\gamma)$ is carried out by use of the quantum-mechanical density matrix, and the result is found to agree well with the classical result. As $D^{(\ell)}_{m'm}$ describes the transformation of a spherical tensor $T^{(\ell)}$ from the molecular framework to the space-fixed framework, orientational averaging of the tensor can also be effected. Orientation-averaged spin Hamiltonians are developed by using this formalism, and are found to consist, in general, of a sum of terms, in each of which appears a scalar product of the molecule-fixed tensors $T^{(\ell)}$ and the molecule-fixed electric moment tensors, multiplied by the scalar product of space-fixed electric field tensors with space-fixed nuclear operator tensors. The tensors $T^{(\ell)}$ considered are the chemical shift and indirect spin-spin tensors, each with $\ell = 0, 1, 2$, and the magnetic dipolar interaction and intramolecular electric field gradient tensors, each with $\ell = 2$. Diagonalization of the orientation-averaged spin Hamiltonian is described for a general two-spin system in which the Zeeman energy is large and small, respectively, as compared with the electric quadrupole energy. Matrix elements of the nuclear

operators are given for the coupled and uncoupled scheme of two nuclei. The spherical tensor formalism is used throughout.

M. W. P. Strandberg

B. EXPANSION OF VELOCITY SURFACES IN SPHERICAL HARMONICS

The velocity of sound in an elastic medium is given by the roots of a 3×3 secular equation

$$D\left[\Gamma_{\substack{i\\j}}(\theta,\phi) - \lambda\delta_{\substack{i\\j}}\right] = 0.$$

A method has been developed for expressing the branches of this secular equation in an analytic approximation. The method consists of a least-squares fit of a finite sum of basis functions of the proper symmetry.

$$\lambda_a(\theta,\phi) = \sum_{\ell,\,m} W_\ell^m(\theta,\phi)\, C_{\ell,\,m}^a,$$

where $a = 1, 2, 3$ and denotes the branch.

The secular equation has been solved for all points on a grid covering a fundamental symmetry region. The three values of λ at each of these points have been used to determine the value of the C's. The "longitudinal" branch has the greatest λ at all points and is easily separated from the two transverse branches; however, the two "transverse" branches are not easily separable. In certain regions the two curves develop sharp corners and come quite close to one another. Two types of fitting were tried to account for this type of behavior. In the first, we attempted to fit the sharp corners with a small number of terms. In the second, we ignored the sharp corners and assumed that the curves continued smoothly, so that one part of one curve joins onto that of the other. This results in an intersection of the two surfaces which in general does not really exist.

The first approximation is referred to as nonintersecting, and the second as intersecting. Neither method is accurate close to the points of singularity, but the volume over which the error exists should be small.

The velocity of sound as a function of direction in a crystal will have the same symmetry as the crystal. Since our interest is in quartz and sapphire, it was necessary to choose linear combinations that would be invariant under D_{3d}. Table III-1 lists the unnormalized functions that were used. Also listed are the special harmonics proportional to these functions. Table III-2 lists the coefficients for the fourteen basic functions.

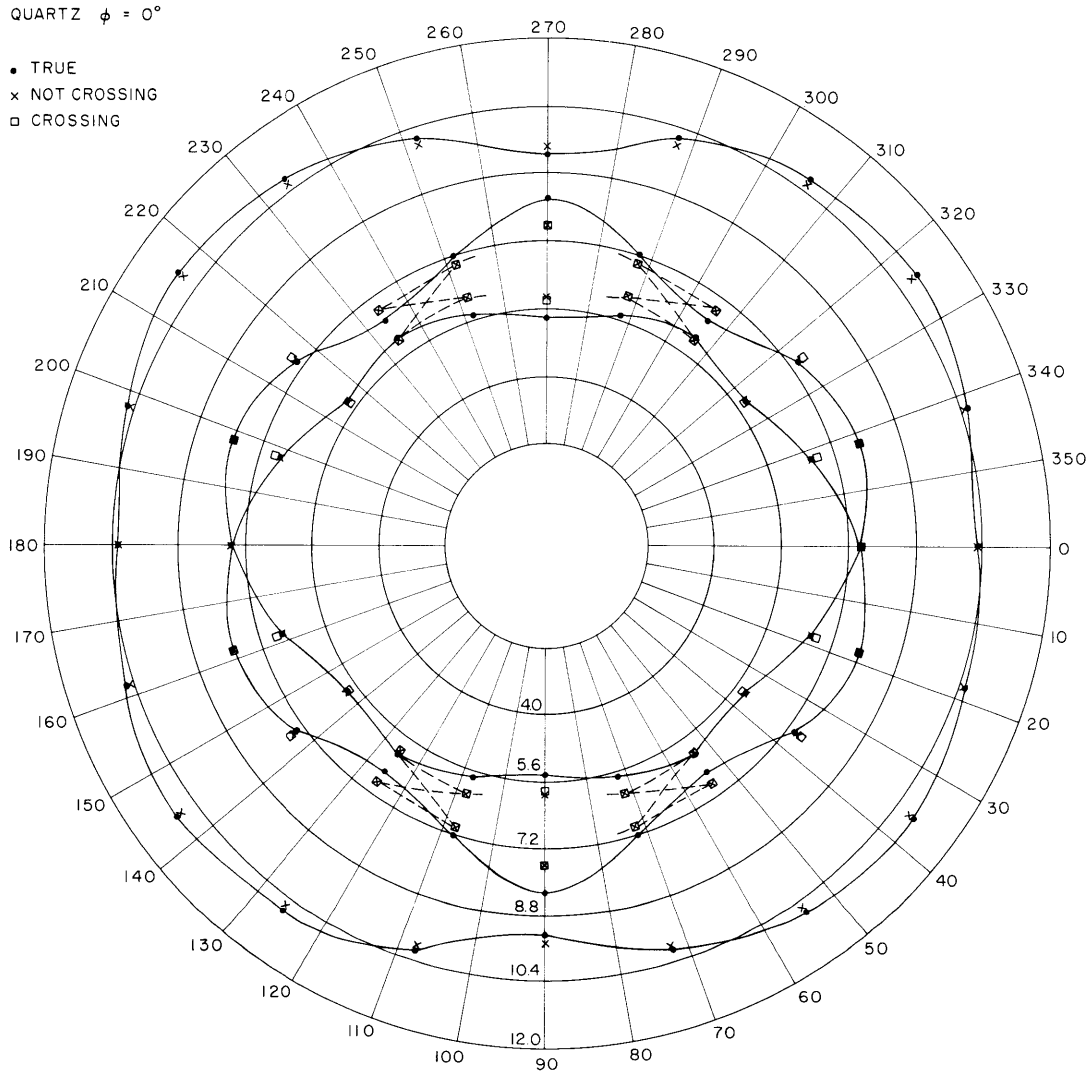

Fig. III-1. True values of λ in crossing and noncrossing approximations for quartz.

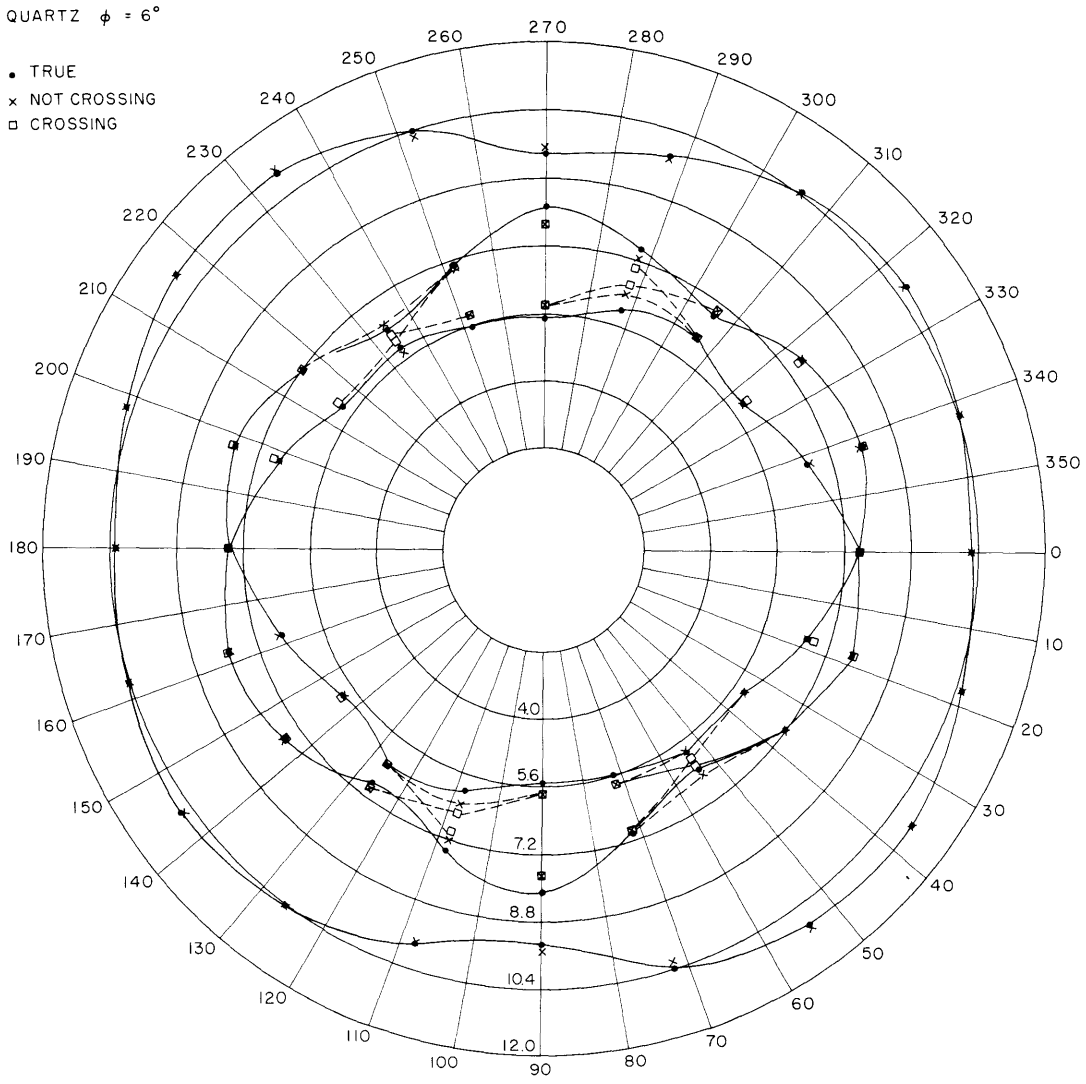

Fig. III-1. Continued.

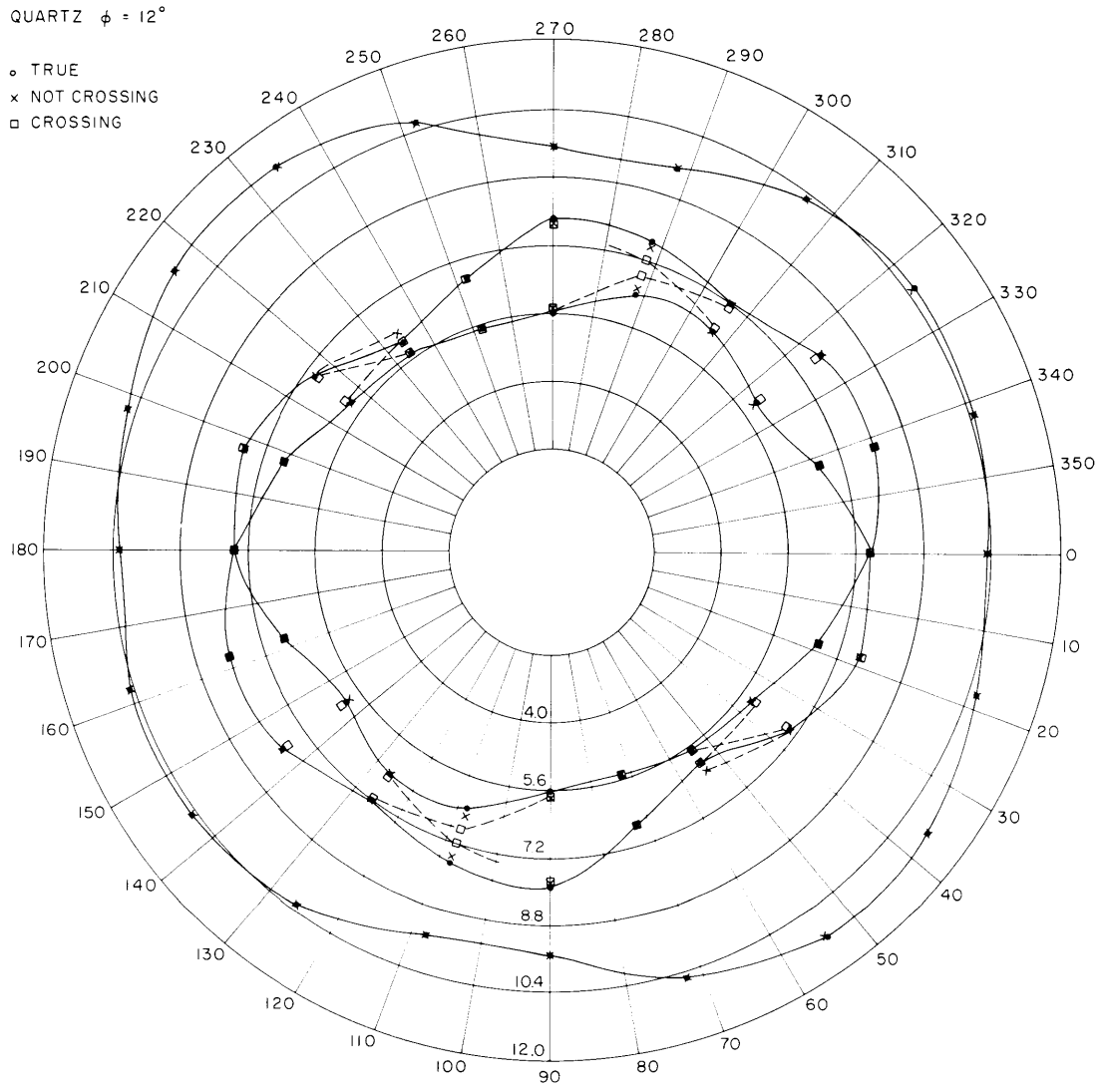

Fig. III-1. Continued.

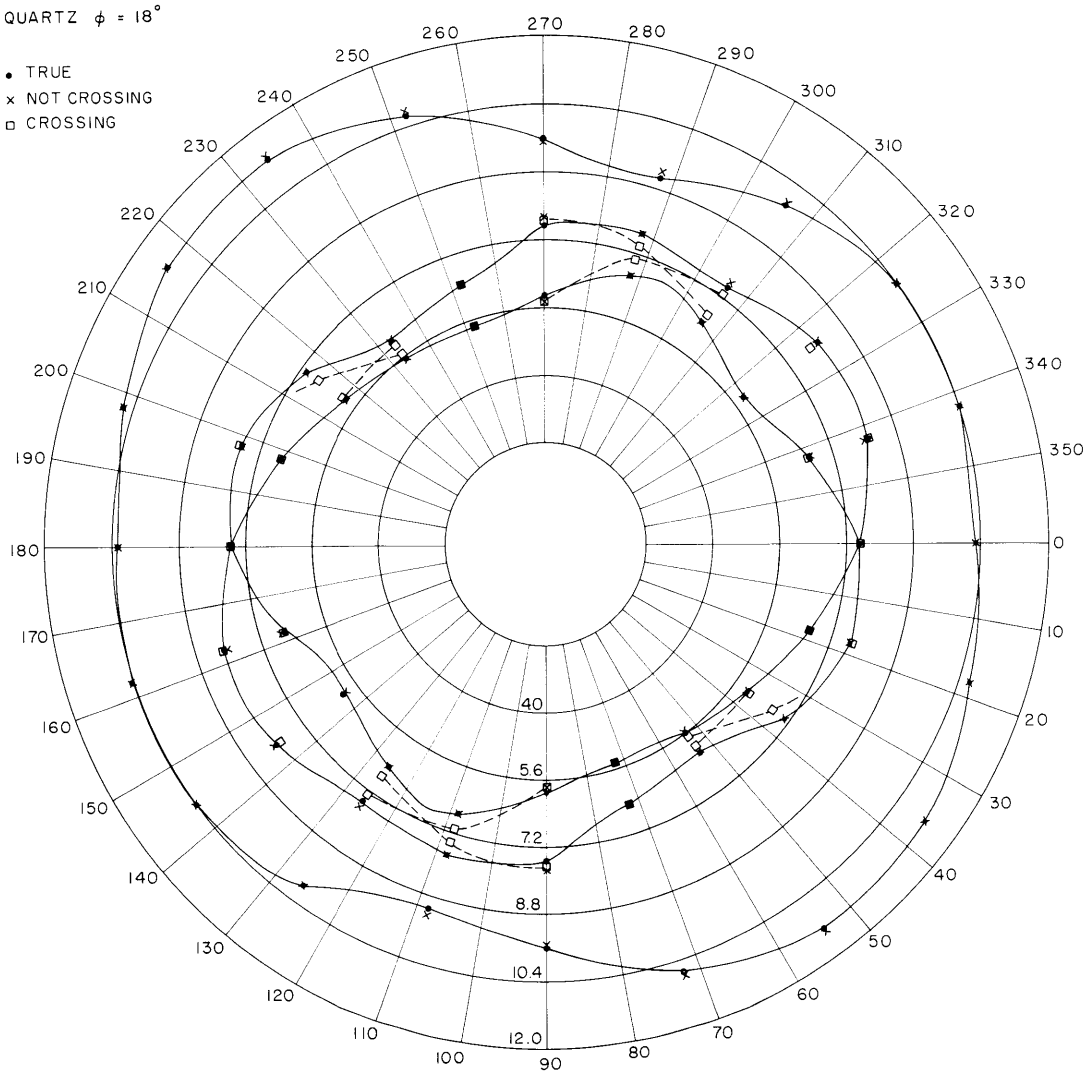

Fig. III-1. Continued.

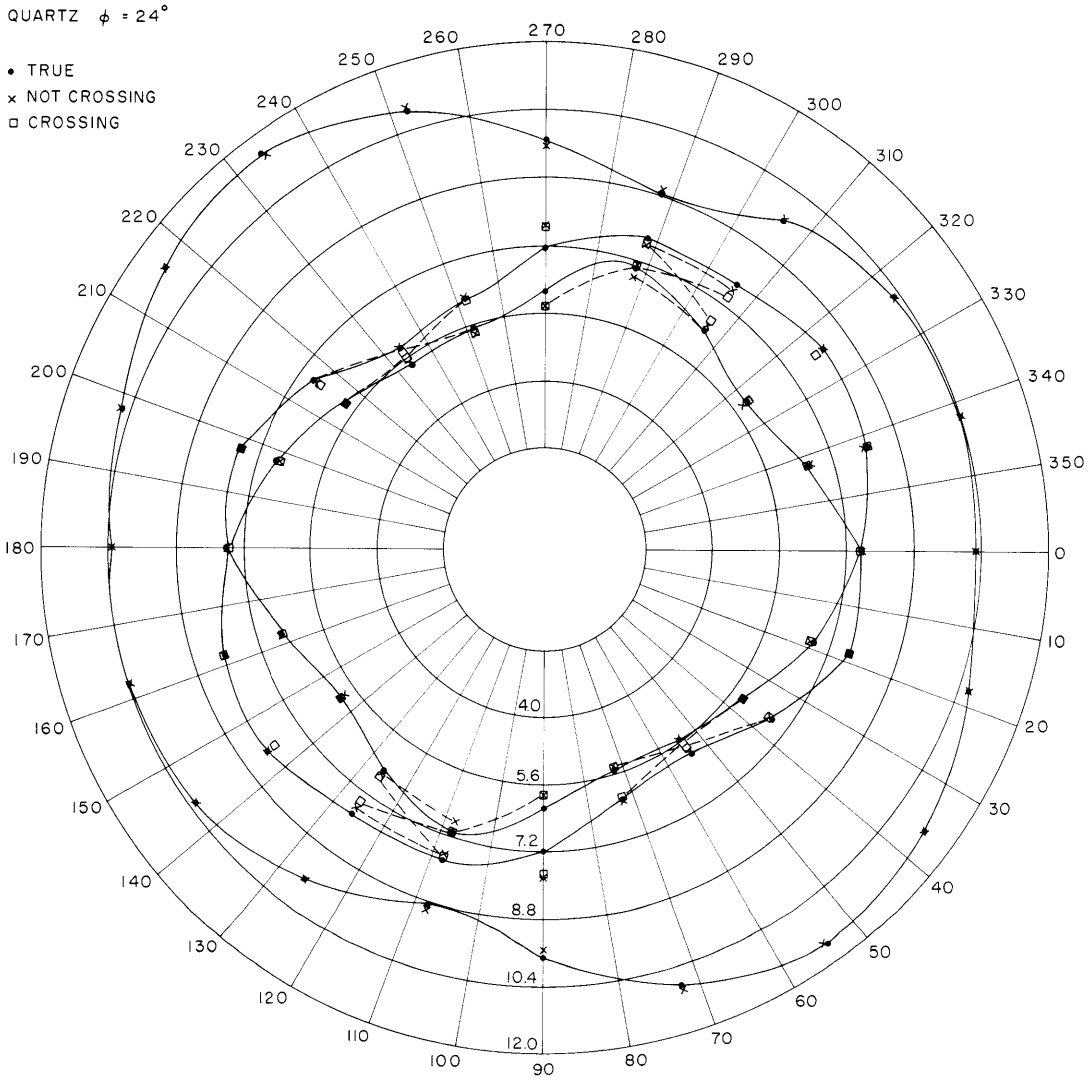

Fig. III-1. Continued.

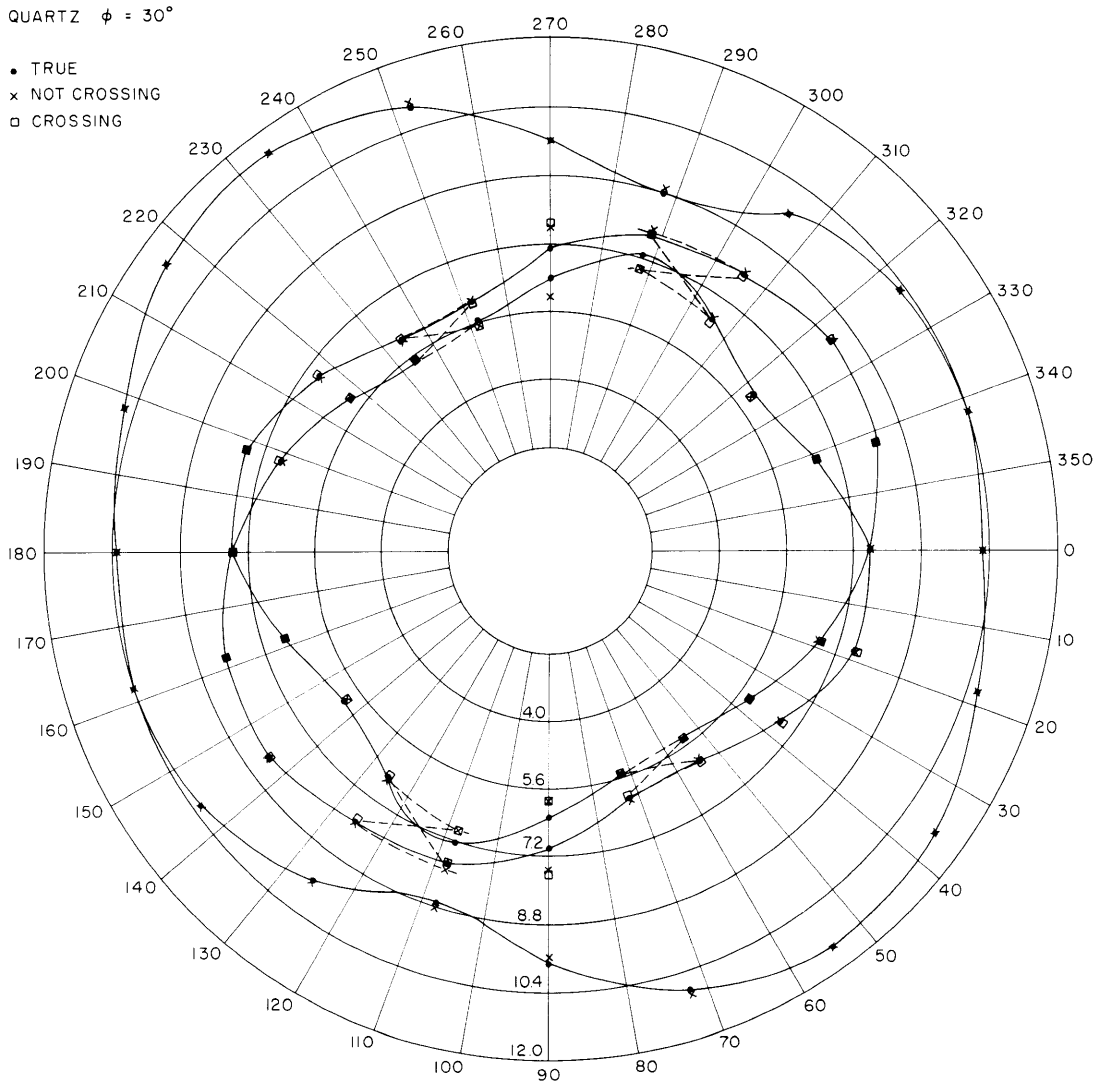

Fig. III-1. Concluded.

Table III-1. Basic functions.

No.	Spherical Harmonic	Function
1	Y_o^o	1
2	Y_2^o	$\frac{1}{2}(3\cos^2\theta - 1)$
3	Y_4^o	$\frac{1}{8}(35\cos^4\theta - 30\cos^2\theta + 3)$
4	$Y_4^3 + Y_4^{-3}$	$(-1)(105)\sin^3\theta\cos\theta\sin(3\phi)$
5	Y_6^o	$\frac{1}{16}[-5 + 105\cos^2\theta - 315\cos^4\theta + 231\cos^6\theta]$
6	$Y_o^3 + Y_o^{-3}$	$\sin^3\theta\left[\frac{945}{2}\cos\theta - \frac{3465}{2}\cos^3\theta\right]\sin(3\phi)$
7	$Y_o^6 - Y_o^{-6}$	$1039\sin^6\theta\sin(6\phi)$
8	Y_8^o	$\frac{1}{128}[35 - 1260\cos^2\theta + 6930\cos^4\theta - 12012\cos^6\theta + 6435\cos^8\theta]$
9	$Y_8^3 + Y_8^{-3}$	$\frac{1}{128}\left[-(6930)\,4!\cos\theta + (12012)\frac{(6!)}{3!}\cos^3\theta - (6435)\frac{8!}{5!}\cos^5\theta\right]\sin^3\theta\sin(3\phi)$
10	$Y_8^6 - Y_8^{-6}$	$\frac{1}{128}\left[-(12012)\,6! + (6435)\frac{8!}{2!}\cos^8\theta\right]\sin^6\theta\sin(6\phi)$
11	Y_{10}^o	$-\frac{63}{256}\left[1 - 55\cos^2\theta + \frac{1430}{3}\cos^4\theta - 1430\cos^6\theta + \frac{12155}{7}\cos^8\theta - \frac{46189}{63}\cos^{10}\theta\right]$
12	$Y_{10}^3 + Y_{10}^{-3}$	$\frac{63}{256}\left[11440\cos\theta - (1430)\frac{6!}{3!}\cos^3\theta + 12155\frac{8!}{5!}\cos^5\theta - \frac{46189}{63}\cos^7\theta\right][\sin^3\theta]\sin(3\phi)$
13	$Y_{10}^6 - Y_{10}^{-6}$	$\frac{63}{256}\left[1430\,(6!) - \frac{12155}{7}\frac{8!}{2!}\cos^2\theta + \frac{46189}{63}\frac{10!}{4!}\cos^4\theta\right]\sin^6\theta\sin(6\phi)$
14	$Y_{10}^9 + Y_{10}^{-9}$	$-\frac{46186}{256}(10!)\cos\theta\sin^9\theta\sin(9\phi)$

Table III-2. Coefficients for basic functions.

A. Quartz

No.	Longitudinal	Noncrossing No. 1	Transverse No. 2	Crossing No. 1	Transverse No. 2
1	1.02694	.72560	.61241	.67827	+.65973
2	.083864	.037667	.023577	.15148	-.090196
3	-.076627	.071489	.045001	-.037285	.15374
4	.093571	-.32044	.26547	.28025	-.30981
5	.0034625	-.066357	.067744	-.0073593	+.0087664
6	.049406	-.16469	.13402	.141368	-.15908
7	$.92088\times10^{-6}$	$.87029\times10^{-6}$	$-.18051\times10^{-5}$	$-.20201\times10^{-5}$	$.10852\times10^{-5}$
8	-.0044750	.0021378	-.0019092	-.020501	.020743
9	.013518	-.045298	.036945	.038948	-.043734
10	$.10264\times10^{-6}$	$-.16674\times10^{-6}$	$.65002\times10^{-7}$	$-.042531\times10^{-6}$	$.30074\times10^{-6}$
11	-.00033281	-.0093415	.0098118	-.0098324	.010285
12	.0015990	-.0053456	.0043559	.0045828	-.0051524
13	$-.33161\times10^{-8}$	$-.829158\times10^{-8}$	$.12186\times10^{-7}$	$-.65656\times10^{-7}$	$.69553\times10^{-7}$
14	$.60771\times10^{-10}$	$-.55847\times10^{-10}$	$.22882\times10^{-10}$	$.11470\times10^{-9}$	$-.14769\times10^{-9}$

B. Sapphire

No.	Longitudinal	Transverse No. 1	Noncrossing No. 2
1	2.30464	1.5426	1.20511
2	.14889	.087645	.065676
3	-.089904	.11134	.036036
4	.010070	-.038211	.032754
5	.0030266	-.14666	.15966
6	.0094793	-.022792	.012749
7	$.42283\times10^{-6}$	$.36553\times10^{-5}$	$-.40537\times10^{-5}$
8	.0098677	-.055929	.044110
9	.0024740	-.006100	.0034896
10	$.47100\times10^{-7}$	$-.22437\times10^{-6}$	$.17464\times10^{-6}$
11	-.0037530	-.012597	.015833
12	.00029974	-.00073529	.00041982
13	$.17323\times10^{-7}$	$-.23263\times10^{-7}$	$.774918\times10^{-8}$
14	$.58666\times10^{-10}$	$-.14354\times10^{-10}$	$-.32633\times10^{-10}$

Figure III-1 shows the true values of λ in the crossing and noncrossing approximations for quartz.

S. R. Reznek

C. RUBY CROSS RELAXATION

The nonexponential behavior of electron cross relaxation in dilute ruby, which was reported in Quarterly Progress Report No. 72 (pages 14-15), has been explained in terms of thermal contact between the Cr^{3+} electron dipole-dipole reservoir and the larger Al^{27} nuclear Zeeman reservoir of the Al_2O_3. Figure III-2 shows the coupling scheme. The basic principle is that the electron dipole-dipole reservoir[1,2] is in better thermal contact with the Al^{27} nuclei than with the rest of the electron-spin system.

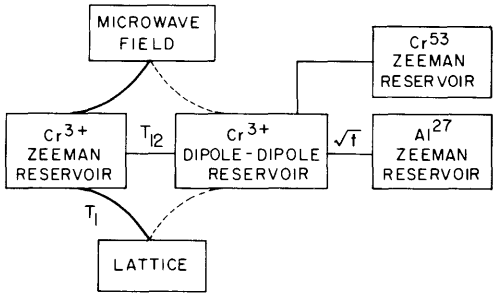

Fig. III-2. Electron and nuclear spin-coupling scheme in dilute ruby.

For two-quantum cross relaxation, which is fast, the bottleneck is the coupling between the dipole-dipole reservoir and the Al^{27} nuclei. The observed square root of time law represents nuclear spin diffusion.

For three-quantum cross relaxation, which is slower, the cross-relaxation process determines the rate, and a good exponential is observed.

R. L. Kyhl

References

1. J. Philippot, Phys. Rev. 133, A471 (1964).
2. J. Jeener, H. Eisendrath, and R. Van Steenwinkel, Phys. Rev. 133, A478 (1964).